

# Liquid Crystalline Assembly of a Diblock Rod–Coil Polymer Based on Poly(ethylene oxide) and Its Complexes with $\text{LiCF}_3\text{SO}_3$

Myongsoo Lee\* and Nam-Keun Oh

Department of Chemistry, Yonsei University, Sinchon 134, Seoul 120-749, Korea

Hwan-Koo Lee and Wang-Cheol Zin

Department of Materials Science and Engineering, Pohang University of Science and Technology, Pohang 790-784, Korea

Received September 20, 1995; Revised Manuscript Received May 14, 1996<sup>®</sup>

**ABSTRACT:** The rod–coil polymer of ethyl 4-[4'-oxy-4-biphenylcarbonyloxy]-4'-biphenylcarboxylate with poly(ethylene oxide) with a degree of polymerization of 12 (**12-4**) was observed to exhibit a microphase-separated lamellar structure with nanoscale dimension and to melt into a layered smectic A mesophase. The complexes of **12-4** with 0.05–0.8 mol of  $\text{LiCF}_3\text{SO}_3$  per ethylene oxide unit of a molecule were also prepared in order to investigate mesomorphic phase changes of **12-4** upon complexation. An abrupt mesophase change was observed for the entire range of salt concentrations. The complexes with 0.05–0.2 mol of  $\text{LiCF}_3\text{SO}_3$  display an enantiotropic smectic A phase as their highest temperature mesophase. From the complex with 0.2 mol of  $\text{LiCF}_3\text{SO}_3$ , an enantiotropic cubic phase is induced and a smectic A phase disappears at the complex with 0.25 mol of  $\text{LiCF}_3\text{SO}_3$ , which displays a cubic mesophase only. The complex with 0.3 mol of  $\text{LiCF}_3\text{SO}_3$  also exhibits an enantiotropic cubic phase; however, it exhibits a cylindrical micellar mesophase as its highest temperature mesophase, contrary to the complexes with up to 0.25 mol of  $\text{LiCF}_3\text{SO}_3$ . The complexes with 0.4–0.7 mol of  $\text{LiCF}_3\text{SO}_3$  exhibit only a cylindrical micellar mesophase, and the complex with higher salt concentration becomes amorphous. These results, characterized by a combination of differential scanning calorimetry, optical polarized microscopy, and X-ray scattering experiments, are discussed.

## Introduction

The tendency for a given molecule to display a particular liquid crystalline supramolecular structure is related to its shape, aspect ratio, and dipolar properties.<sup>1</sup> Rod-shaped molecules with one or two flexible tails generally assemble into nematic or smectic phases, whereas disk-shaped molecules tend to display columnar phases. While the guiding principle of shape is extensively used in the design of liquid crystals, little attention has been paid to generating the desired mesophases with rod–coil molecules which are macromolecular analogues for low molar mass smectogens. The covalent linkage between a rigid rod and an elongated flexible coil may be an attractive way of creating new supramolecular structures, because the resulting rod–coil molecules are able to segregate incompatible (for example, rigid rod and flexible coil) segments of individual molecules.

Theoretical works have shown that various supramolecular structures such as nematic, layered smectic, and cylindrical phases could be induced depending on the relative volume fraction of coil in rod–coil diblock systems.<sup>2–5</sup> For example, rod–coil molecules with a sufficiently short flexible coil exhibit a nematic phase. With increasing coil length, block microsegregation occurs due to the large chemical differences between stiff rod and flexible coil segments to form a layered smectic assembly. As the coil length is further increased, molecular layers may collapse into discrete cylindrical micellar structures. Experimental works have also been performed on systems consisting of molecular rod blocks coupled to polyisoprene<sup>6,7</sup> or poly(isoprene-*block*-styrene) coil blocks to form linear diblocks.<sup>8</sup> The supramolecular structure in the rod–coil systems was observed to vary from lamellar to micellar microphase-separated domains as coil volume fraction is increased, although

molecular order within the rigid rod blocks was not reported.<sup>7</sup>

To date, little work has been carried out on rod–coil diblock systems containing the poly(ethylene oxide) coil. Poly(ethylene oxide) has several advantages, particularly due to its complexation capability with alkali metal cations, which can induce various liquid crystalline supramolecular structures. A recent publication on poly(ethylene ether) with flexible side groups has shown that complexation of polymer backbones with  $\text{LiClO}_4$  induced a smectic lamellar mesophase from a crystalline phase of uncomplexed polymer.<sup>9</sup> Experimental works on taper-shaped molecules containing oligo(ethylene oxide) have also demonstrated that complexation of the molecules with alkali metal trifluoromethanesulfonate could induce a hexagonal columnar mesophase.<sup>10–12</sup>

It is in this context that we have synthesized rod–coil polymers, consisting of a molecular rod and poly(ethylene oxide) as the coil, and investigated their mesomorphic behaviors.<sup>13</sup> The  $\text{LiCF}_3\text{SO}_3$  complexes of the rod–coil polymer molecule **16-4** (where the rod is ethyl 4-[4'-oxy-4-biphenylcarbonyloxy]-4'-biphenylcarboxylate and the coil is poly(ethylene oxide) with degree of polymerization of 16) have also been characterized by a combination of differential scanning calorimetry (DSC) and thermal optical microscopy. The preliminary results suggested that the complexation of **16-4** with  $\text{LiCF}_3\text{SO}_3$  could induce a cylindrical micellar mesophase from a layered smectic phase of the uncomplexed polymer.

However, in order to elucidate mesophase behavior as a function of salt concentration, a systematic complexation study on a rod–coil diblock systems is required. As an extension of this study, the rod–coil polymer **12-4** (where the rod is ethyl 4-[4'-oxy-4-biphenylcarbonyloxy]-4'-biphenylcarboxylate and the coil is poly(ethylene oxide) with degree of polymerization of 12) has been characterized by both small-angle and

\* To whom correspondence should be addressed.

<sup>®</sup> Abstract published in *Advance ACS Abstracts*, July 15, 1996.

**Table 1. Thermal Transitions of the Complexes of Rod–Coil Polymer 12-4<sup>a</sup>**

complex [LiCF <sub>3</sub> SO <sub>3</sub> ]/[EO]	phase transition (°C) and corresponding enthalpy changes (kJ/mol) <sup>b</sup>	
	heating	cooling
0.00	k 13.8 (46.4) k 135.2 (15.6) s <sub>A</sub> 148.1 (1.85) i k 15.0 (48.6) k 134.4 (14.9) s <sub>A</sub> 147.9 (1.95) i	i 144.4 (1.92) s <sub>A</sub> 128.9 (15.4) k -3.7 (44.4) k
0.05	k -4.8 (17.1) k 126.7 (14.4) s <sub>A</sub> 164.8 (1.97) i k -0.2 (23.8) k 128.6 (13.4) s <sub>A</sub> 162.8 (1.74) i	i 159.6 (1.81) s <sub>A</sub> 125.1 (12.8) k
0.10	g -32 k 114.4 (8.78) s <sub>A</sub> 167.8 (1.51) i k 118.9 (9.27) s <sub>A</sub> 166.7 (1.31) i	i 163.3 (1.25) s <sub>A</sub> 116.6 (9.27) k
0.15	g -30.1 k 100.9 (6.45) s <sub>A</sub> 163.5 (0.92) i g -38 k 107.1 (6.99) s <sub>A</sub> 162.7 (0.83) i	i 158.3 (1.11) s <sub>A</sub> 103.6 (7.24) k -35 g
0.20	g -17 k 93.3 (6.00) OI 131.5 (0.32) s <sub>A</sub> 154.1 (0.68) i g -25 k 100.2 (6.47) OI 135.0 (0.42) s <sub>A</sub> 154.0 (0.54) i	i 145.0 (0.57) s <sub>A</sub> 114.4 (0.19) OI 87.7 (3.96) k -25 g
0.25	g -8 k 92.8 (2.59) OI 137.2 (0.62) i g -14 k 85.0 (1.61) OI 135.6 (0.63) i	i 120.7 (0.66) OI 64.7 (0.47) k -10 g
0.30	g -3 k 87.8 (2.51) OI 120.0 (0.03) M 126.2 (0.24) i g -16 k 80.0 (0.82) OI 117.1 (0.02) M 125.8 (0.15) i	i 118.2 (0.10) M 105.4 (-) <sup>c</sup> OI 57.2 (0.38) k -25 g
0.35	g -12 k 92.1 (3.24) OI 100.1 (0.11) M 124.0 (0.16) i g 4 k 73.0 (1.73) OI (0.25) 125.5 (0.15) i	i 114.2 (0.05) M 87.1 (-) <sup>c</sup> OI 49.7 (0.42) k 5 g
0.40	g -0.5 k 77.1 (3.26) M 120.5 (0.11) i g -4.8 k 74.3 (0.92) M 119.5 (0.21) i	i 108.9 (0.04) M 40.5 (0.04) k 0.3 g
0.50	g -3 k 63.3 (2.13) M 114.5 (0.03) i g -7 k 43.2 (0.02) M 114.9 (0.02) i	i 96.9 (0.02) M -3 g
0.60	g 6 M 92.4 (-) <sup>c</sup> i g 5 M 92.3 (-) <sup>c</sup> i	i 73.1 (-) <sup>c</sup> M -7 g
0.70	g 15 M 74.0 (-) <sup>c</sup> i g 13 M 74.0 (-) <sup>c</sup> i	i 57.2 (-) <sup>c</sup> 10 g
0.80	g 25 i g 27 i	i 22 g

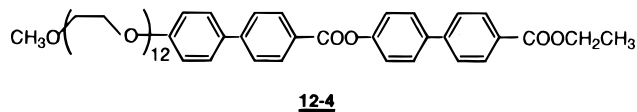
<sup>a</sup> s<sub>A</sub> = smectic A phase, OI = optical isotropic cubic phase, M = cylindrical micellar mesophase, g = glassy phase, k = crystalline phase, i = isotropic phase. Data on the first line are from the first heating and cooling scans. Data on the second line are from the second heating scan. <sup>b</sup> The molecular weight is weight averaged with the amount of LiCF<sub>3</sub>SO<sub>3</sub> present. <sup>c</sup> Data obtained from optical polarized microscopy.

wide-angle X-ray scattering experiments in order to investigate the morphology. The complexes of **12-4** with 0.05–0.8 mol of LiCF<sub>3</sub>SO<sub>3</sub> per ethylene oxide unit of a molecule have also been prepared in order to investigate mesomorphic phase changes of **12-4** upon complexation. The goal of this paper is to describe the morphological character of **12-4** and its phase change upon complexation with LiCF<sub>3</sub>SO<sub>3</sub>. The mesomorphic phase behavior, characterized by a combination of DSC, optical polarized microscopy, and X-ray scattering experiments, is discussed.

## Experimental Section

**Techniques.** A Perkin-Elmer DSC-7 differential scanning calorimeter, equipped with a 1020 thermal analysis controller, was used to determine the thermal transitions, which were reported as the maxima and minima of their endothermic or exothermic peaks, respectively. Glass transition temperatures (*T<sub>g</sub>*) were read at the midpoint of the change in heat capacity. In all cases, heating and cooling rates were 10 °C/min unless otherwise specified. Indium was used as a calibration standard. A Nikon Optiphot 2-pol optical polarized microscope (magnification: 100×) equipped with a Mettler FP 82 hot stage and a Mettler FP 90 central processor were used to observe the thermal transitions and to analyze the anisotropic textures.<sup>14,15</sup> X-ray scattering measurements were performed in transmission mode with nickel-filtered Cu Kα radiation supplied by a Rigaku Denki generator operating at 40 kV and 40 mA. In order to investigate structural changes on heating, the samples were held in an aluminum sample holder which was sealed with windows of 8 μm thick Kapton films on both sides. The samples were heated with two cartridge heaters, and the temperature of the samples was monitored by a thermocouple placed close to the sample. Background scattering correction was made by subtracting the scatterings from the Kapton. The small-angle X-ray scattering measurements were performed with a Kratky camera fitted with an M. Broun linear position sensitive detector. The correction for the slit-length smearing was applied by means of Strobl's algorithm.<sup>16</sup>

**Synthesis of 12-4.** The chemical structure of the rod–coil polymer **12-4** is outlined in Chart 1. The details of the

**Chart 1. Chemical Structure of the Rod–Coil Polymer 12-4**

synthesis and characterization of **12-4** were reported in a previous publication.<sup>13</sup>

**Preparation of Complexes of 12-4.** Complexes of **12-4** with lithium triflate were prepared by mixing solutions of **12-4** (10 mg/mL) in dry methylene chloride with an appropriate volume of 0.724 mmol/mL salt in dry acetonitrile solution. This was followed by slow evaporation of the solvent under reduced pressure at room temperature and subsequent drying in a vacuum oven at 60 °C until a constant weight was attained.

## Results and Discussion

The observations of this work were made on rod–coil polymer **12-4** and its complexes with 0.05–0.8 mol of LiCF<sub>3</sub>SO<sub>3</sub> per ethylene oxide unit of **12-4**. The chemical structure of **12-4** is shown in Chart 1. The phase behavior of the rod–coil polymer and its complexes with lithium triflate was characterized by a combination of techniques consisting of differential scanning calorimetry (DSC), thermal optical polarized microscopy, and both small-angle and wide-angle X-ray scattering experiments. The DSC traces obtained during the first and subsequent heating and the first and subsequent cooling scans are identical. The experimental data collected from both scans are summarized in Table 1. However, the second heating and first cooling DSC scans will be presented in more detail. Figure 1 shows DSC traces of the second heating scans and of the first cooling scans of the rod–coil polymer **12-4** and its complexes with 0.05–0.8 mol of lithium triflate per ethylene oxide unit of **12-4**.

As shown in Figure 1, **12-4** exhibits a crystalline melting which corresponds to the poly(ethylene oxide)

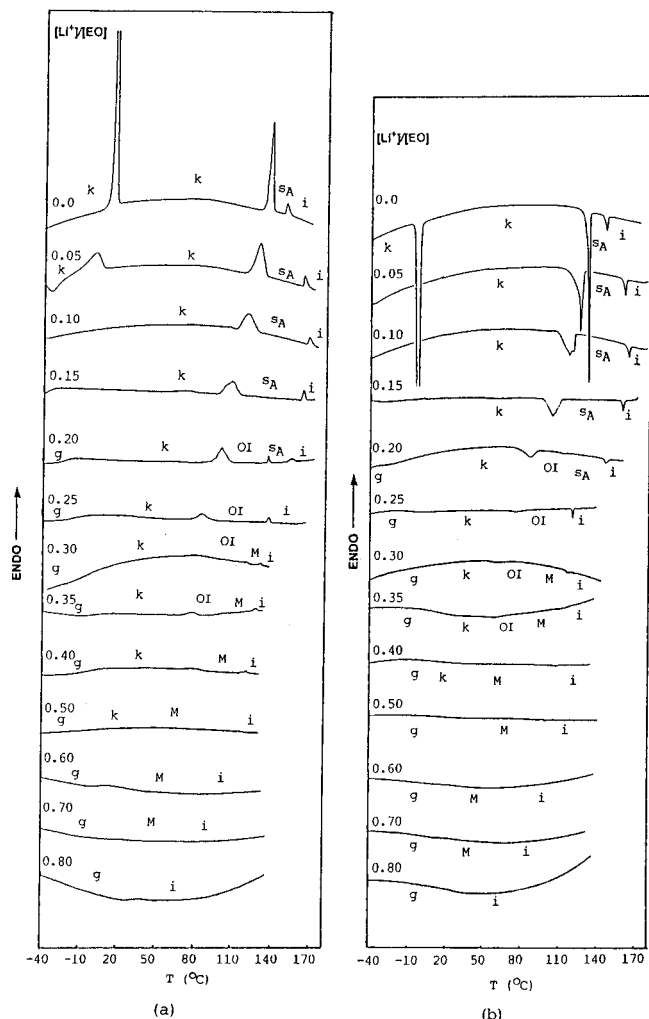


**Figure 1.** DSC traces recorded during the second heating scan (a) and first cooling scan (b) of the complexes of **12-4** with  $\text{LiCF}_3\text{SO}_3$ .

coil block followed by a crystalline phase of the rod block which, in turn, undergoes melting into a smectic A mesophase, regardless of the thermal history of the sample. The hydrophilic coil and hydrophobic rod segments are believed to be highly incompatible and, therefore, becomes microphase separated even in the melt state, although the molecular weights of each block are very low. This gives rise to the two crystalline melting transitions which correspond to each block and the formation of a smectic A phase. This trend has also been confirmed for a related rod-coil polymer, and the higher crystalline melting transition has been verified to correspond to the rod block in a previous publication.<sup>13</sup> Optical microscope observations of this compound are consistent with this behavior. Transition from an isotropic liquid at 144 °C can be seen by the rapid formation of batonnets which merge into a focal conic fanlike texture with pseudoisotropic areas indicating a smectic A phase (Figure 2).<sup>14,15</sup>

In order to investigate the microphase-separated morphology, X-ray experiments have been performed with **12-4** before and after the melting transition temperature of the rod segments. The small-angle X-ray diffraction pattern of **12-4** in the crystalline state displays three reflections with scattering vectors of 0.94 (very strong), 1.89, and 2.83  $\text{nm}^{-1}$  as shown in Figure 3a, while a series of sharp strong reflections is observed in the wide-angle diffraction pattern shown in Figure

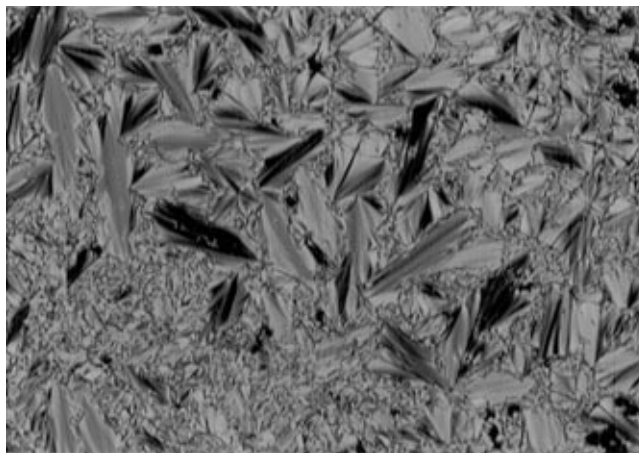


**Figure 2.** Representative optical polarized micrograph (100 $\times$ ) of the texture exhibited by the  $s_A$  mesophase of **12-4** at 142 °C on the cooling scan.

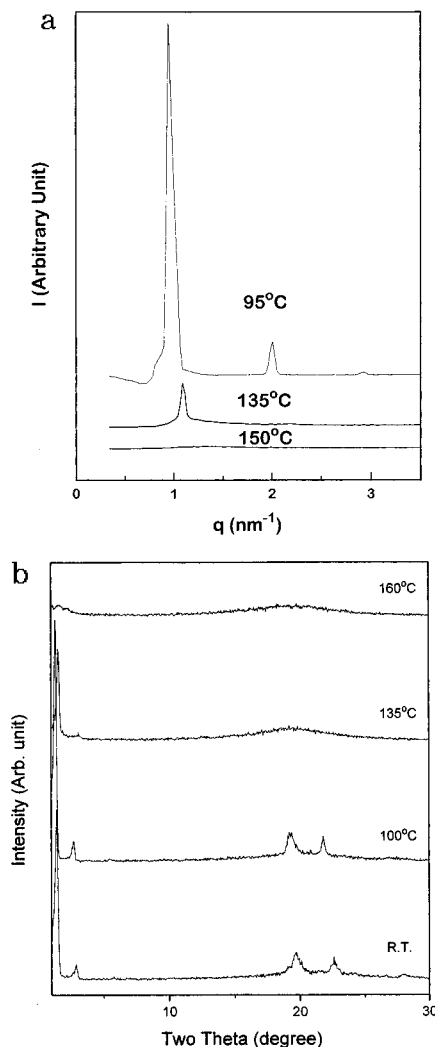


**Figure 3.** (a) Desmeared SAXS intensity for the rod-coil polymer **12-4** plotted against  $q (=4\pi \sin \theta/\lambda)$ . The curves show the data obtained at 95, 135 and 150 °C. (b) Wide-angle diffraction patterns of the rod-coil polymer **12-4**. The curves show the data obtained at room temperature, 100, 135, and 160 °C.

3b. This indicates that the crystalline phase of **12-4** is a lamellar structure with 6.6 nm periodicity. This microphase-separated structures with nanoscale dimensions of <10 nm have also been observed for rod-coil diblock systems containing polyisoprene oligomers.<sup>6,7</sup>

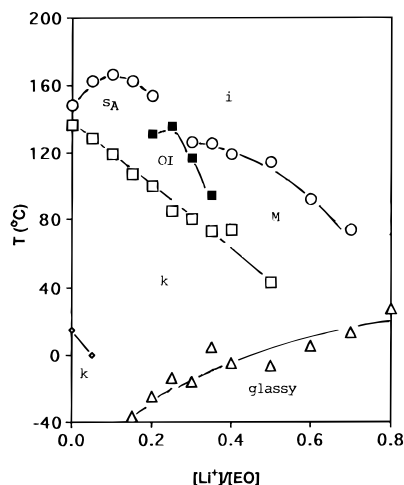


**Figure 4.** Dependence of phase transition temperatures of the complexes of **12-4** with lithium triflate on the  $[\text{LiCF}_3\text{SO}_3]/[\text{EO}]$ . Data from second DSC heating scan; ( $\Delta$ )  $T_g$ ; ( $\diamond$ )  $T_{k-k}$ ; ( $\square$ )  $T_m$ ; ( $\blacksquare$ )  $T_{\text{OI-sA}}$ ,  $T_{\text{OI-i}}$ , or  $T_{\text{OI-M}}$ ; ( $\circ$ )  $T_i$ .

Comparison with the calculated length of a fully extended rod-coil unit of ca. 6.9 nm suggests that the 6.6 nm periodicity arises from monolayers resulting from the phase segregation of rod and coil segments. These results together with DSC data suggest that the microphase-separated rod domains are crystalline while the coil domains are amorphous at 95 °C. In the liquid crystalline phase at 135 °C, a sharp strong reflection and two small peaks are observed in the small-angle region, suggesting a lamellar phase with 5.8 nm periodicity (Figure 3a), while the sharp reflections observed in the wide-angle region disappear and only a diffuse halo is observed, indicating the melting of the aromatic rods (Figure 3b). This supports that **12-4** displays a smectic A mesophase with an interlayer spacing of 5.8 nm. The decrease of interlayer spacing from 6.6 to 5.8 nm upon melting can be explained by the following speculation. The melting of the rod segments gives rise to increasing interfacial surface area and decreasing coil stretching in order to maintain a uniform density, consequently, decreasing the layer thickness. This is supported by the increase in the specific volume of rod segments upon melting, which is calculated to be ~17%.

It has been reported that alkali metal salts are selectively soluble in the polyether segments of a block copolymer exhibiting a microphase-separated morphology.<sup>17</sup> Therefore, alkali metal ion will be selectively dissolved in the microphase-separated poly(ethylene oxide) coil segments of **12-4** through ion-dipole interaction. This results in an increase of the relative volume fraction of the coil compared to that of the rod, which gives rise to a novel supramolecular structure. In this respect, we have investigated the phase change of **12-4** on complexation with  $\text{LiCF}_3\text{SO}_3$ .

The complex with 0.05 mol of  $\text{LiCF}_3\text{SO}_3$  per ethylene oxide unit of **12-4** exhibits two crystalline melting transitions followed by a smectic A phase on heating. On cooling, the crystalline melting transition which corresponds to the coil block does not appear within this range of temperatures, probably due to a supercooling. Complexes of **12-4** with 0.1–0.2 mol of  $\text{LiCF}_3\text{SO}_3$  display only a crystalline melting which corresponds to the rod block and an enantiotropic smectic A mesophase regardless of the thermal history. The dependence of the phase transitions of **12-4** and its complexes with  $\text{LiCF}_3\text{SO}_3$  on the  $[\text{LiCF}_3\text{SO}_3]/[\text{ethylene oxide}]$  determined from the second heating DSC scans is plotted in Figure 4.

The temperature associated with the mesomorphic-isotropic transition increases up to the complex with 0.10 mol of  $\text{LiCF}_3\text{SO}_3$  per ethylene oxide unit and then decreases, and, consequently the mesophase disappears at the complex with 0.8 mol of  $\text{LiCF}_3\text{SO}_3$ . At the same time, both the crystal melting transitions show a decrease. As a result, the thermal stability of the smectic A phase increases with increasing salt concentration up to 0.10 mol of  $\text{LiCF}_3\text{SO}_3$ . This can be attributed to enhanced rigidity of the poly(ethylene oxide) layer through the cooperative complexation of the added salts with the rod-coil polymer in the layer structure.<sup>18</sup> The enhanced thermal stability of a mesophase via complexation was also confirmed for a hexagonal columnar mesophase induced by taper-shaped molecules.<sup>10–12</sup> The decrease of the isotropization temperature in the complexes with concentration higher than 0.15 mol of  $\text{LiCF}_3\text{SO}_3$  can be explained by the presence of ester oxygen of the rod blocks. At higher salt concentrations, a little ionic species may be inserted into the rod segments through ion-dipole interactions between the ester oxygen of the rod segments and lithium cation, which produces a steric effect that hinders molecular packing. This could result in a large decrease in the isotropic transition temperature with increasing salt concentration.

The complexes with 0.20–0.35 mol of  $\text{LiCF}_3\text{SO}_3$  are very interesting because they exhibit a thermodynamically stable optical isotropic mesophase. As shown in Figures 1 and 4, the complex with 0.20 mol of  $\text{LiCF}_3\text{SO}_3$  melts into an optical isotropic phase, and further heating gives rise to a smectic A mesophase. On cooling from the smectic A mesophase, dark, isotropic rectangular and rhombic areas with straight edges appear and these regions then grow until the entire field of view is dark, which are characteristic of the cubic phase.<sup>14,15</sup> When the optical isotropic phase was submitted to pressure by touching the cover glass, no flashing or birefringence was observed between crossed polarizers. This indicates that the optical isotropic phase is not a pseudoisotropic one with a homeotropic arrangement. The complex with 0.25 mol of  $\text{LiCF}_3\text{SO}_3$  exhibits a similar phase behavior except that the mesophase above the cubic phase does not exist. On melting of the complexes with 0.3 and 0.35 mol of  $\text{CF}_3\text{SO}_3$ , a cubic phase is also formed; however, further heating gives rise to a new mesophase showing pseudofocal conic domains. A representative texture of the cubic phase of the complex with 0.3 mol of  $\text{LiCF}_3\text{SO}_3$  is shown in Figure 5. The cubic phase is rare in thermotropic liquid crystalline molecules and has been observed in only a few systems such as biphenyl carboxylic acid derivatives with lateral nitro and cyano groups,<sup>15,19</sup> azoxybenzene derivatives,<sup>20</sup> two chain diols,<sup>21</sup> silver thiolates, and several biforked mesogens.<sup>22,23</sup> Although molecular models for the structure of the cubic phase have been proposed,<sup>24,25</sup> they are still a controversial subject.<sup>26–28</sup>

In contrast to the phase behavior of the complexes with up to 0.2 mol of  $\text{LiCF}_3\text{SO}_3$ , the complexes with 0.3–0.6 mol of  $\text{LiCF}_3\text{SO}_3$  do not exhibit an SA phase but they display an enantiotropic cylindrical micellar mesophase. On cooling from the isotropic liquid, first, a platelet-like growing of the texture can be observed with a final development of pseudofocal conic domains as shown in Figure 6. This is characteristic of a conventional disordered columnar mesophase exhibited by discotic liquid crystals.<sup>29</sup> As shown in Figure 4, the transition temperatures associated with the cylindrical-

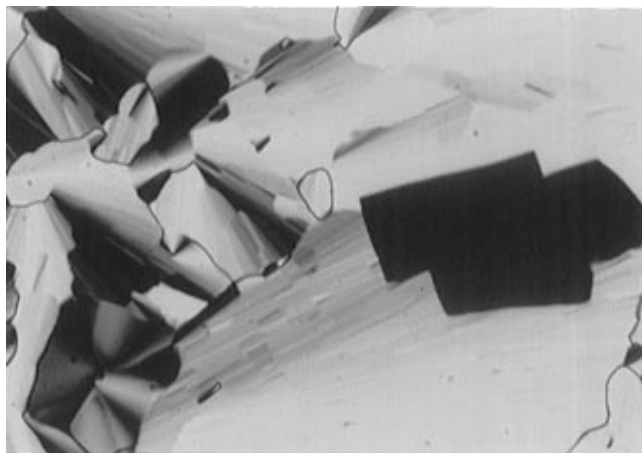


**Figure 5.** Representative optical polarized micrograph (100 $\times$ ) of the texture of the dark area with straight edges exhibited by the optical isotropic cubic phase of the complex of **12-4** with 0.3 mol of  $\text{LiCF}_3\text{SO}_3$  at 105  $^\circ\text{C}$  on the cooling scan.

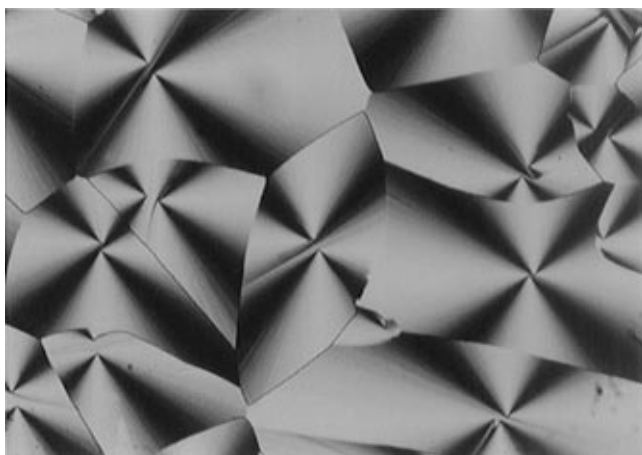


**Figure 6.** Representative optical polarized micrograph (100 $\times$ ) of the texture exhibited by the cylindrical micellar mesophase of the complex of **12-4** with 0.3 mol of  $\text{LiCF}_3\text{SO}_3$  at 110  $^\circ\text{C}$  on the cooling scan.

isotropic phase decrease and crystallization is suppressed with increasing salt concentration; consequently, the complex becomes amorphous at the complex with 0.8 mol of  $\text{LiCF}_3\text{SO}_3$ .

For morphological investigation of these complexes, both small-angle and wide-angle X-ray scattering experiments have been performed with the complex with 0.4 mol of  $\text{LiCF}_3\text{SO}_3$  at various temperatures. Figure 7 presents SAXS patterns of the complex with 0.4 mol of  $\text{LiCF}_3\text{SO}_3$  performed at various temperatures. In the crystalline phase at 67  $^\circ\text{C}$ , the complex displays several strong wide-angle reflections. In the small-angle X-ray region, the crystalline phase exhibits the intense fundamental and its second and third harmonic reflections, respectively, at scattering vectors of 0.94 (very strong), 1.82, and 2.77  $\text{nm}^{-1}$ . Therefore, the crystalline phase of the complex with 0.4 mol of  $\text{LiCF}_3\text{SO}_3$  is generated by layers of 6.8 nm periodicity. Interestingly, this interlamellar distance is very close to the 6.6 nm periodicity shown in the crystalline phase of the uncomplexed polymer. This result indicates that the complexation of **12-4** with  $\text{LiCF}_3\text{SO}_3$  does not influence the volume change of the coil segments in the crystalline phase, most probably due to strong ion-dipole interactions between the poly(ethylene oxide) coil and lithium cation. This is also supported by density measurement experiments, which show the density increase from 1.23

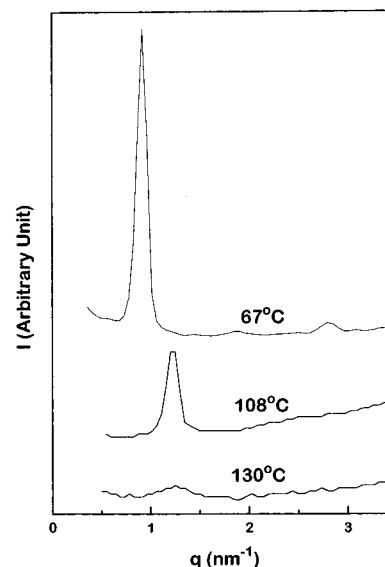


**Figure 7.** Desmeared SAXS intensity for the complex of **12-4** with 0.4 mol of  $\text{LiCF}_3\text{SO}_3$  plotted against  $q$  ( $=4\pi \sin \theta/\lambda$ ). The curves show the data obtained at 67, 108, and 130  $^\circ\text{C}$ .

to 1.37  $\text{g}/\text{cm}^3$  on complexation of **12-4** with 0.4 mol of  $\text{LiCF}_3\text{SO}_3$ .

In the liquid crystalline phase at 108  $^\circ\text{C}$ , a single reflection is observed at a scattering vector of 1.25  $\text{nm}^{-1}$  and the lattice constant is 5.0 nm as shown in Figure 7, while the wide-angle X-ray experiment shows only a broad halo in the range of  $\sim 4.5$   $\text{\AA}$ . The periodicity of the complex is significantly reduced to 5.0 nm in comparison to that (5.7 nm) in the smectic A phase of **12-4**. The large reduction of periodicity together with optical polarized microscope observations suggests that the mesophase exhibited by the complex is a disordered cylindrical micellar mesophase which is analogous to those predicted recently.<sup>2</sup>

It is well known that associated ionic species or ion pairs increase with increasing temperature or increasing salt concentration in polymer-salt complex systems.<sup>30</sup> Therefore, the enhanced thermal motions of the molecules, including the increased associated ionic species on melting of the complex, cause the flexible coils grafted onto their top and bottom surfaces in the monolayer structure to fan out into a larger region of space. Consequently, this spatial requirement of the coil segments leads to the transformation of the lamellar structure in the crystalline phase changes into a cylindrical micellar mesophase as shown in Figure 8. The micellar structure allows more volume and less coil stretching. This spreading out of the poly(ethylene oxide) chains is reflected in the large reduction observed for the complex with 0.4 mol of  $\text{LiCF}_3\text{SO}_3$  from the layer periodicity in the solid (6.8 nm) to the intermicellar distance in the micellar mesophase (5.0 nm). Additional experiments which support these assumptions are in progress.

The results presented in this paper suggest that complexation of the rod-coil polymer containing poly(ethylene oxide) with  $\text{LiCF}_3\text{SO}_3$  can induce a cylindrical micellar mesophase from a lamellar smectic A mesophase as well as a lamellar crystalline phase as shown in Figure 8. The existence of a cylindrical micellar mesophase is in contrast with the normal behavior of conventional calamitic mesogens, which show the lamellar smectic and/or nematic phase. Lamellar and cylindrical micellar mesophases for a given compound are

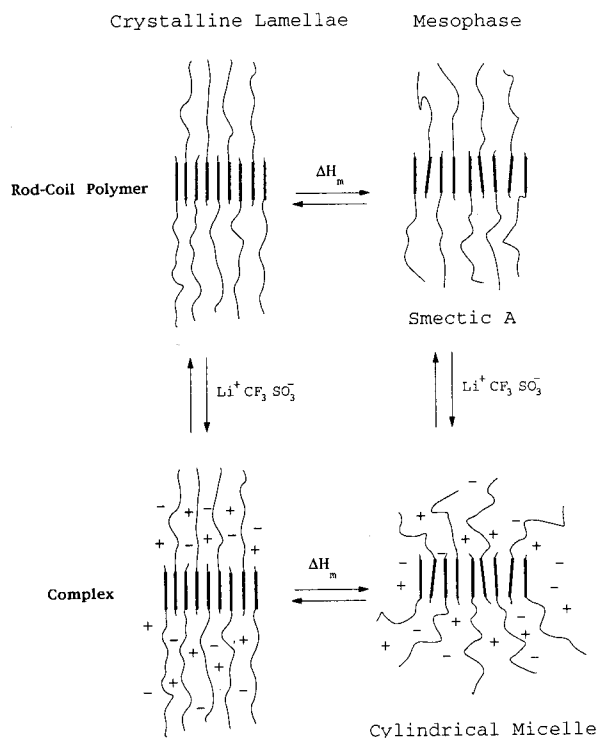


**Figure 8.** Schematic representation of the possible models of the structures of **12-4** in the crystalline solid and the lamellar smectic A mesophase and of the complex in the crystalline solid and the cylindrical micellar mesophase.

commonly found in lyotropic liquid crystals<sup>31,32</sup> and also contribute to the thermal behavior of some amphiphilic molecules such as silver thiolates<sup>33</sup> and the biforked molecules.<sup>34,35</sup> On the other hand, columnar mesophases are usually induced by disk-shaped mesogens and consequently prone to this kind of stacking.<sup>36</sup> Therefore, the system discussed here is an unusual case of a calamitic mesogenic system.

X-ray measurements have also been carried out in an isotropic liquid phase of both **12-4** and the complex as shown in Figure 3a (curve at 150 °C) and 7 (curve at 130 °C). Both **12-4** and the complex exhibit a small broad peak at about 5.0 nm even in the isotropic liquid phase. This is a high-temperature feature for conventional block and graft copolymers which exhibit a microphase-separated morphology<sup>37</sup> and is most probably due to the presence of dynamic density inhomogeneity in the liquid state.<sup>38</sup>

Apparently, the lamellar smectic A structure observed in the uncomplexed rod-coil polymer and the complexes with up to 0.2 mol of  $\text{LiCF}_3\text{SO}_3$  is still the most efficient packing of melt chains because the volume fraction of coil parts is not large enough.<sup>3,4</sup> At higher concentration of  $\text{LiCF}_3\text{SO}_3$ , however, the volume fraction of coil segments increases, presumably due to the increase of the ionic species in the coil segments through selective solvation.<sup>38</sup> The system becomes unstable due to a large space crowding; consequently, the lamellar structure of the rod-coil polymer will break apart into cylindrical micelles.<sup>2</sup> The main advantage of these micelles relative to lamellae is that the coils grafted onto their top and bottom surfaces are able to fan out into a larger region of space, presumably to reduce the thermodynamic stretching penalty (Figure 8). This might explain qualitatively the phase behavior of this rod-coil system.

In conclusion, the rod-coil polymer **12-4** was observed to organize into a microphase-separated lamellar structure with nanoscale dimension and a layered smectic A

mesophase on melting. Upon complexation of **12-4** with  $\text{LiCF}_3\text{SO}_3$ , a dramatic change of phase behavior was observed through an entire range of salt concentrations. The complexes display successively lamellar smectic A, cubic, and cylindrical micellar mesophases with increasing concentration of  $\text{LiCF}_3\text{SO}_3$ . The temperature associated with the mesomorphic-isotropic transition increases up to the complex with 0.10 mol of  $\text{LiCF}_3\text{SO}_3$  per ethylene oxide unit and then decreases. Consequently the mesophase disappears at the complex with 0.8 mol of  $\text{LiCF}_3\text{SO}_3$ . In particular, transformation of a smectic A phase into a cylindrical micellar assembly by simple complexation of the rod-coil polymer system with a calamitic mesogen is promising. These results provide a useful approach to a large variety of fundamental investigations and technological applications.

**Acknowledgment.** Financial support of this work by the Ministry of Education, Republic of Korea (BSRI-94-3422), through the Research Institute of Basic Sciences of Yonsei University is gratefully acknowledged.

## References and Notes

- (1) Chandrasekhar, S. In *Liquid Crystals*, 2nd ed.; Cambridge University Press: Cambridge, 1992.
- (2) Williams, D. R. M.; Fredrickson, G. H. *Macromolecules* **1992**, *25*, 3561.
- (3) Semenov, A. N.; Vasilenko, S. V. *Sov. Phys.-JETP (Engl. Transl.)* **1986**, *63*, 70.
- (4) Semenov, A. N. *Mol. Cryst. Liq. Cryst.* **1991**, *209*, 191.
- (5) Halperin, A. *Macromolecules* **1990**, *23*, 2724.
- (6) Radzilowski, L. H.; Wu, J.; Stupp, S. I. *Macromolecules* **1993**, *26*, 879.
- (7) Radzilowski, L. H.; Stupp, S. I. *Macromolecules* **1994**, *27*, 7747.
- (8) Stupp, S. I.; Lee, M.; Son, S.; Li, L. S.; Kesser, M. *Polym. Prepr. (Am. Chem. Soc., Div. Polym. Chem.)* **1993**, *43*(1), 184.
- (9) Dias, F. B.; Voss, J. P.; Batty, S. V.; Wright, P. V.; Ungar, G. *Makromol. Chem., Rapid Commun.* **1994**, *15*, 961.
- (10) Percec, V.; Heck, J.; Tomazos, D.; Falkenberg, F.; Blackwell, H.; Ungar, G. *J. Chem. Soc., Perkin Trans. 1* **1993**, 2799.
- (11) Percec, V.; Tomazos, D.; Heck, J.; Blackwell, H.; Ungar, G. *J. Chem. Soc., Perkin Trans. 2* **1994**, 31.
- (12) Percec, V.; Heck, J.; Johansson, G.; Tomazos, D. *Makromol. Chem., Symp.* **1994**, *77*, 237 and references cited therein.
- (13) Lee, M.; Oh, N.-K. *J. Mater. Chem.*, in press.
- (14) Demus, D.; Richter, L. *Textures of Liquid Crystals*; Verlag Chemie: Weinheim, 1978.
- (15) Gray, G. W.; Goodby, J. W. *Smectic Liquid Crystals. Textures and Structures*; Leonard Hill: Glasgow, 1984.
- (16) Strobl, G. R. *Acta Crystallogr., Sect. A* **1970**, *A26*, 367.
- (17) (a) Gray, F. M. In *Solid Polymer Electrolytes, Fundamentals and Technological Applications*; VCH Publishers: Weinheim, 1993; Chapter 6. (b) MacCallum, J. R.; Tomlin, A. S.; Vincent, C. A. *Eur. Polym. J.* **1986**, *22*, 787.
- (18) Keller, A.; Ungar, G.; Percec, V. In *Advances in Liquid Crystalline Polymers*; Ober, C. K., Weiss, R. A., Eds.; ACS Symposium Series 435; American Chemical Society: Washington, DC, 1990; p 308.
- (19) Gray, G. W.; Jones, B.; Marson, F. *J. Chem. Soc.* **1957**, 393.
- (20) Yano, S.; Mori, Y.; Kutsumizu, S. *Liq. Cryst.* **1991**, *9*, 907.
- (21) Lattermann, G.; Staufer, G. *Mol. Cryst. Liq. Cryst.* **1990**, *191*, 199.
- (22) Tihm, N. H.; Destrade, C.; Levelut, A. M.; Malthete, J. *J. Phys. (Les. Ulis. Fr.)* **1986**, *47*, 553.
- (23) Hendrikx, Y.; Levelut, A. M. *Mol. Cryst. Liq. Cryst.* **1988**, *165*, 233.
- (24) Luzzati, V.; Spagt, P. A. *Nature* **1967**, *215*, 701.
- (25) Diele, S.; Brand, P.; Sackmann, H. *Mol. Cryst. Liq. Cryst.* **1972**, *17*, 163.
- (26) Guillon, D.; Skoulios, A. *Europhys. Lett.* **1987**, *3*, 79.
- (27) Etherington, G.; Langley, A. J.; Leadbetter, A. J.; Wang, X. *J. Liq. Cryst.* **1988**, *3*, 155.
- (28) Demikhov, E. I.; Dolganov, V. K.; Korshunov, V. V.; Demus, H. *Liq. Cryst.* **1988**, *3*, 161.
- (29) Destrade, C.; Foucher, P.; Gasparoux, H.; Tinh, N. H. *Mol. Cryst. Liq. Cryst.* **1984**, *106*, 121.
- (30) (a) Huang, W.; Frech, R. *Polymer* **1994**, *35*, 235. (b) Schantz, S.; Sandahl, J.; Borjesson, L.; Torell, L. M.; Stevens, J. R.

- Solid State Ionics* **1988**, 28–30, 1047. (c) Torell, L. M.; Santz, S. In *Polymer Electrolyte Reviews*; MacCullum, J. R., Vincent, C. A., Eds.; Elsevier: London, 1989; Vol. 2.
- (31) Luemann, B.; Finkelmann, H. *Colloid Polym. Sci.* **1987**, 265, 506.
- (32) Hoffmann, H. *Adv. Mater.* **1994**, 6, 116.
- (33) Baena, M. J.; Espinet, P.; Lequerica, M. C.; Levulet, A. M. *J. Am. Chem. Soc.* **1992**, 114, 4182.
- (34) Fang, Y.; Levulet, A. M.; Destrade, C. *Liq. Cryst.* **1990**, 7, 265.
- (35) Destrade, C.; Tinh, N. H.; Roubineau, A.; Levulet, A. M. *Mol. Cryst. Liq. Cryst.* **1988**, 159, 163.
- (36) Praefcke, K.; Marquardt, P.; Kohne, B.; Luz, Z.; Poupko, R. *Liq. Cryst.* **1991**, 9, 711.
- (37) Roe, R. J.; Fishkis, M.; Chang, J. C. *Macromolecules* **1981**, 14, 1091.
- (38) (a) de Gennes, P.-G. *J. Phys. (Les Ullis, Fr.)* **1970**, 31, 235.  
(b) Leibler, L. *Macromolecules* **1980**, 13, 1602.

MA951418Y